PHYSICAL REVIEW B **84**, 180410(R) (2011)

# Single-ion anisotropy in Haldane chains and the form factor of the $O(3)$ nonlinear sigma model

Shunsuke C. Furuya,[1] Takafumi Suzuki,[2] Shintaro Takayoshi,[1] Yoshitaka Maeda,[3] and Masaki Oshikawa[1]

[1]*Institute for Solid State Physics, University of Tokyo, Kashiwa 277-8581, Japan*

[2]*Research Center for Nano-Micro Structure Science and Engineering, Graduate School of Engineering, University of Hyogo, Himeji 671-2280, Japan*

[3]*Analysis Technology Center, Fujifilm Corporation, Kanagawa 250-0193, Japan*

(Received 27 October 2011; published 21 November 2011)

We consider spin-1 Haldane chains with single-ion anisotropy, which exists in known Haldane chain materials. We develop a perturbation theory in terms of anisotropy, where the magnon-magnon interaction is important even in the low-temperature limit. The exact two-particle form factor in the $O(3)$ nonlinear sigma model leads to quantitative predictions on several dynamical properties, including the dynamical structure factor and electron-spin-resonance frequency shift. These agree very well with numerical results, and with experimental data on the Haldane chain material $Ni(C_5H_{14}N_2)_2N_3(PF_6)$.

DOI: 10.1103/PhysRevB.84.180410 PACS number(s): 75.10.Jm, 75.30.Gw, 76.30.−v

One-dimensional quantum spin systems are an ideal subject to test sophisticated theoretical concepts against experimental reality.[1] One of the best examples is the Haldane gap problem. Haldane predicted in 1983 (Ref. 2) that the standard Heisenberg antiferromagnetic (HAF) chain $\mathcal{H} = J\sum_j \boldsymbol{S}_j \cdot \boldsymbol{S}_{j+1}$ has a nonzero excitation gap and exponentially decaying spin-spin correlation function for an integer spin quantum number $S$. It has been long known that the HAF chain with $S = 1/2$ is exactly solvable by a Bethe ansatz, and that it has gapless excitations and the power-law spin-spin correlation function. While the same model cannot be solved exactly for $S \geqslant 1$, Haldane's prediction was rather unexpected and surprising at the time.

Haldane's argument was based on the mapping of the HAF chain to the $O(3)$ nonlinear sigma model (NLSM), which is a field theory defined by the action

$$\mathcal{A}_0 = \frac{1}{2g}\int dt\,dx\left[\frac{1}{v}(\partial_t \boldsymbol{n})^2 - v(\partial_x \boldsymbol{n})^2\right] + i\theta Q, \qquad (1)$$

where $g = 2/S$ is coupling constant, $v$ is the spin-wave velocity, $\theta = 2\pi S$, and $Q = (1/4\pi)\int dt\,dx\,\boldsymbol{n}\cdot\partial_t\boldsymbol{n}\times\partial_x\boldsymbol{n}$ is an integer-valued topological charge. The field $\boldsymbol{n}(x)$ is related to the spin $\boldsymbol{S}_j$ via $\boldsymbol{S}_j \approx (-1)^j\sqrt{S(S+1)}\,\boldsymbol{n}(x) + \boldsymbol{L}(x)$, where $\boldsymbol{L}(x) = \boldsymbol{n}\times\partial_t\boldsymbol{n}/g$. The field $\boldsymbol{n}$ has a constraint $\boldsymbol{n}^2 = 1$. For a half integer $S$, the topological term $i\theta Q$ should be kept. However, for an integer $S$, the topological term $i\theta Q = 2\pi i \times$ (integer) is irrelevant and it suffices to drop $i\theta Q$ in Eq. (1). The $O(3)$ NLSM without the topological term is a massive field theory, which implies that the integer $S$ HAF chain (Haldane chain) has a nonzero gap and a finite correlation length. The Haldane's conjecture is now confirmed by a large body of theoretical, numerical, and experimental studies.[3] Moreover, the $O(3)$ NLSM is also useful in describing integer $S$ HAF chains.

There are various complications in real materials. A Haldane chain material generally has a single-ion anisotropy (SIA): $\mathcal{H}' = \sum_j[D(S_j^z)^2 + E\{(S_j^x)^2 - (S_j^y)^2\}]$. This interaction is important, for example, for electron-spin-resonance (ESR) measurements. ESR is a useful experimental probe which can detect even very small anisotropies. In other words, the anisotropic interaction is the key to understanding a rich store of ESR experimental data. However, the theory of ESR is not sufficiently developed for many systems, including Haldane chains, leaving many experimental data not being understood. In order to fully exploit the potential of ESR, accurate formulation of the SIA in Haldane chains is required.

The SIA can be treated as a perturbation since it is usually small compared to the isotropic exchange interaction $J$. In $O(3)$ NLSM language, the perturbation is written as

$$\mathcal{H}' = S(S+1)\int dx[D(n^z)^2 - E\{(n^x)^2 - (n^y)^2\}], \qquad (2)$$

which spoils the integrability of the $O(3)$ NLSM. Several simple calculations have been done based on the Landau-Ginzburg (LG) model.[4,5] When the elementary excited particles (magnons) are dilute, the interaction between magnons may be ignored. If this is the case, the system is effectively described by a much simpler theory of free massive magnons (the LG model).[4] However, the description by the LG model is not accurate and, furthermore, it is phenomenological.[6] Even in the low-energy limit, where the free-magnon approximation is supposed to be exact, it is not the case with respect to the evaluation of Eq. (2). This is because the perturbation (2) creates and annihilates two magnons at the same point; in such a situation, interaction among the magnons is indeed important even when the average density of magnons in the entire system is infinitesimal. Therefore, correct handling of the SIA in the $O(3)$ NLSM framework requires a proper inclusion of the magnon interaction.

In this Rapid Communication, we present such a formulation utilizing the integrability of the $O(3)$ NLSM. The effects of interaction are encoded in the form factors of operators. The form factors in integrable field theories can be determined by the consistency with the exact $S$ matrices and several additional axioms.[7–9] Form factor expansion (FFE) is particularly powerful in massive field theories such as the $O(3)$ NLSM, because the higher-order contributions survive only above the higher-energy thresholds.[10] The leading contribution to the FFE of Eq. (2) is given by the two-particle form factor. The FFE shows an excellent agreement with the correlation function of $(S^z)^2$ numerically obtained in the $S = 1$ HAF chain, demonstrating the importance of the interaction. At

 

the same time, the renormalization factor for the SIA (2) is determined by the fitting of the numerical data. Furthermore, we discuss two applications to physical problems of interest: the split of triplet magnons in the dynamical structure factor and the ESR shift in the $S = 1$ HAF chain with SIA. We find very good agreement with numerical results in both applications, and with experimental data on the ESR shift, without introducing any extra fitting parameter.

A single-magnon excitation can be parametrized by the rapidity $\theta$, so that its energy and wave number are given, respectively, as $\Delta_0 \cosh\theta$ and $(\Delta_0/v)\sinh\theta$, where $\Delta_0 = 0.41J$ is the Haldane gap. Because of interactions among magnons, the $S$ matrix of $O(3)$ NLSM has a complicated structure.[11] The one-particle form factor of an operator $O$ is defined as a matrix element which connects the ground state $|0\rangle$ to a one-particle state $|\theta_1,a_1\rangle$ ($a_1 = 1,2,3$), namely, $F_{\mathcal{O}}(\theta_1,a_1) \equiv \langle 0|\mathcal{O}|\theta_1,a_1\rangle$. And the $n$-particle form factor is defined as $F_{\mathcal{O}}(\theta_1,a_1;\theta_2,a_2;\ldots;\theta_n,a_n) \equiv \langle 0|\mathcal{O}|\theta_1,a_1;\theta_2,a_2;\ldots;\theta_n,a_n\rangle$, where this $n$-particle state is normalized as $\langle\theta_1',a_1';\ldots;\theta_n',a_n'|\theta_1,a_1;\ldots;\theta_n,a_n\rangle = (4\pi)^n\delta_{a_1',a_1}\ldots\delta_{a_n',a_n}\delta(\theta_1'-\theta_1)\ldots\delta(\theta_n'-\theta_n)$.

The FFE of the fundamental field $n^a$, which corresponds to (a staggered part of) the spin operator $S^a$, has often been studied. The leading contribution to the FFE is the one-particle form factor $F_{n^a}(\theta_1,a_1)$. Because $n^a$ is odd under the transformation $\boldsymbol{n} \to -\boldsymbol{n}$, the next order contribution comes from the three-particle form factor, which gives small corrections to the spin-spin correlation function.[12–14] On the other hand, the composite operator $(S^a)^2$, which is of our central interest, has been less studied. Since it is proportional to $(n^a)^2$ and even under the reversal $\boldsymbol{n} \to -\boldsymbol{n}$, the leading contribution to the FFE comes from the two-particle form factor $F_{(n^a)^2}(\theta_1,a_1;\theta_2,a_2)$. We note that the exact two-particle form factor of the antisymmetric field $\boldsymbol{L}(x)$ in the $O(3)$ NLSM has been applied to describe the uniform part of the spin-spin correlation function of HAF chains.[14–16] Including the renormalization factors for spin operators, which are undetermined at this point, we have

$$F_{S^a}(\theta_1,a_1) = \sqrt{Z}\,\delta_{a,a_1}, \tag{3}$$

$$F_{(S^a)^2}(\theta_1,a_1;\theta_2,a_2) = -iZ_2\,\delta_{a_1,a_2}(3\delta_{a,a_1}-1)\psi_2(\theta_1-\theta_2). \tag{4}$$

The two-particle form factor (4) receives contributions from higher-order terms in the FFE of $S^a$, and cannot be determined by Eq. (3) alone. Thus $Z_2$ is a parameter independent of $Z$.

We have the constraint $\sum_{a=1,2,3}(S^a)^2 = 2$ on the composite operator. From this constraint and the $O(3)$ symmetry, it follows that $\sum_{a=1,2,3} F_{(S^a)^2}(\theta_1,3;\theta_2,3) = \langle 0|\theta_1,3;\theta_2,3\rangle = 0$, which is satisfied by (4). Integral representation of $\psi_2(\theta)$ is given in Ref. 17 for $O(N)$ NLSM with a general integer $N$. For $N = 3$, it reads

$$\psi_2(\theta) = \sinh\frac{\theta}{2}\exp\left[\int_0^\infty \frac{d\omega}{\omega}e^{-\pi\omega}\frac{\cosh[(\pi+i\theta)\omega]-1}{\sinh(\pi\omega)}\right].$$

This integral can be analytically carried out to give

$$\psi_2(\theta) = \frac{i}{2}(\theta-\pi i)\tanh\frac{\theta}{2}. \tag{5}$$

Determination of the renormalization factors $Z$ and $Z_2$ requires numerical calculations. In order to test the validity of the FFE for $(S^a)^2$ and further to determine $Z_2$, we computed the equal-time correlation function $\langle 0|[S^z(r)]^2[S^z(0)]^2|0\rangle$ by the infinite time-evolving block decimation (iTEBD) method,[18] as shown in Fig. 1.

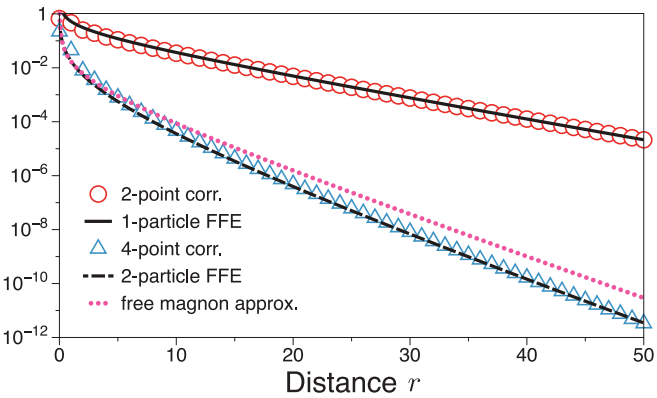


FIG. 1. (Color online) Numerically calculated spin-spin correlation $(-1)^r\langle 0|S^z(r)S^z(0)|0\rangle$ (circles) and the correlation $\langle 0|[S^z(r)]^2[S^z(0)]^2|0\rangle - 4/9$ (triangles) are compared with FFEs (6) with $Z = 1.26$ (solid curve) and the connected part of (7) with $Z_2 = 0.24$ (dashed curve). The free-magnon approximation (dotted curve) cannot fit the correlation function of $(S^z)^2$.

FFE is derived by inserting the identity $\hat{1} = \sum_{n=0}^\infty P_n$, where the $P_n$'s are the projection operators to the $n$-particle subspace of the Fock space, defined by $P_0 = |0\rangle\langle 0|$ and $P_n = \frac{1}{n!}\sum_{a_1,\ldots,a_n}\int\frac{\prod_j d\theta_j}{(4\pi)^n}|\theta_1,a_1;\ldots;\theta_n,a_n\rangle\langle\theta_1,a_1;\ldots;\theta_n,a_n|$ for $n \geqslant 1$. In the leading nonvanishing order, we find

$$(-1)^r\langle 0|S^z(r)S^z(0)|0\rangle \approx Z\int\frac{d\theta}{4\pi}e^{i\Delta_0 r\sinh\theta/v}, \tag{6}$$

$$\langle 0|[S^z(r)]^2[S^z(0)]^2|0\rangle - \frac{4}{9} \approx 3{Z_2}^2\int\frac{d\theta_1 d\theta_2}{(4\pi)^2}|\psi_2(\theta_1-\theta_2)|^2 \times e^{i\Delta_0 r(\sinh\theta_1+\sinh\theta_2)/v}. \tag{7}$$

$Z = 1.26$ was given in Ref. 15 by comparing a numerically obtained spin-spin correlation function with the LG model. Concerning the spin-spin correlation function, the LG model is equivalent to the lowest-order FFE (6); our iTEBD calculation also reproduces the result of Ref. 15. On the other hand, to the best of our knowledge, $Z_2$ has not been determined previously.

As shown in Fig. 1, the lowest order of FFE (7) shows an excellent agreement with the numerical data; the fit also determines

$$Z_2 = 0.24. \tag{8}$$

Since we used the known values of the Haldane gap $\Delta_0 = 0.41J$ and the spin-wave velocity $v = 2.49J$ (Ref. 19) for $S = 1$, the renormalization factor $Z_2$ is the only fitting parameter.

In contrast to the FFE (7), the LG model, which ignores interaction among magnons, shows discrepancy with the numerical data, as also shown in Fig. 1. To illustrate the effect of the interaction, let us discuss the asymptotic long-distance behavior of Eqs. (6) and (7). When $r \to +\infty$, only the behavior of $\psi_2(\theta)$ at $\theta \sim 0$ is relevant in (7). Here we can expand (6) and (7) as $(-1)^r\langle 0|S^z(r)S^z(0)|0\rangle \propto e^{-r/\xi}/\sqrt{8\pi r/\xi}$ and $\langle 0|[S^z(r)]^2[S^z(0)]^2|0\rangle - 4/9 \propto e^{-r/\xi_2}/(4\pi r/\xi_2)$. In a relativistic field theory, the inverse correlation length is equivalent

to the lowest excitation energy created by the operator; in fact, $\xi = v/\Delta_0$. Furthermore, in the LG model,[4] $\xi_2 = \xi/2$ should hold. This is because the composite field $(n^a)^2$ creates two particles, and $O(3)$ NLSM does not contain any bound states.[20] Thus the excitation energy for the two-particle creation would be twice the magnon mass ($2\Delta_0$), implying $\xi_2 = \xi/2$. However, the actual numerical data are inconsistent with this relation: $\xi_2 = 2.75 < \xi/2 = 3.01$. This discrepancy is attributed to the interaction between magnons. Since $(n^a)^2$ creates two magnons *at the same point*, the actual excitation energy is larger than $2\Delta_0$, resulting in $\xi_2 < \xi/2$.

With the full determination of the two-particle form factor (4), we turn to a discussion of the dynamical structure factor (DSF) at $T = 0$ in Haldane chains with a SIA. The peaks in the DSF reflect the energy of the magnon at a given momentum. Triply degenerate magnon dispersions in the isotropic chain are split due to the SIA. We determine the first-order perturbation to the masses $\Delta_a^{(1)} \equiv \Delta_a - \Delta_0$ in the form-factor perturbation theory (FFPT):[21]

$$\Delta_a^{(1)} \sim \frac{\langle\theta,a|\mathcal{H}'|0,a\rangle}{\langle\theta,a|0,a\rangle}. \tag{9}$$

In fact, both the numerator and the denominator are proportional to $\delta(\theta)$, and Eq. (9) should be understood as the ratio of the coefficients of $\delta(\theta)$. Furthermore, the numerator equals to $F_{\mathcal{H}'}(0,a;\theta-\pi i,a)$ because of the crossing symmetry.[22] Therefore, (9) reads

$$\Delta_x^{(1)} = -\frac{Z_2 v}{2\Delta_0} D - \frac{3Z_2 v}{2\Delta_0} E, \tag{10}$$

$$\Delta_y^{(1)} = -\frac{Z_2 v}{2\Delta_0} D + \frac{3Z_2 v}{2\Delta_0} E, \tag{11}$$

$$\Delta_z^{(1)} = \frac{Z_2 v}{\Delta_0} D. \tag{12}$$

The leading contribution to the $T = 0$ DSF $\mathcal{S}^{aa}(\pi,\omega)$ corresponds to the creation of a single magnon. Therefore, we find

$$\mathcal{S}^{aa}(\pi,\omega) \sim \frac{\pi Z v}{\Delta_a}\delta(\omega - \Delta_a), \tag{13}$$

which has the identical form to the DSF of a system of free particles. This is natural because the population of magnons approaches zero in the $T \to 0$ limit, and thus the interactions are negligible. Nevertheless, we emphasize that the change of the masses as $\Delta_a$ (10)–(12) due to the SIA is affected by the magnon-magnon interaction. Equation (13) implies that the magnon masses $\Delta_a$ can be identified with the peak frequency of DSF at the antiferromagnetic wave vector $q = \pi$. In Fig. 2, we compare the magnon masses $\Delta_a$ extracted from the $T = 0$ DSF peak obtained numerically by the Lanczos method[23] for various values of $D$ (while setting $E = 0$). For small $D$, the numerical data agree very well with the FFPT (10)–(12).

The form of the $T = 0$ DSF (13) leads to another prediction: The ratio of the DSF intensities should obey

$$\frac{\int d\omega\, \mathcal{S}^{zz}(\pi,\Delta_z)}{\int d\omega\, \mathcal{S}^{xx}(\pi,\Delta_x)} = \frac{\Delta_x}{\Delta_z}. \tag{14}$$

This is also confirmed by the Lanczos data as shown in the inset of Fig. 2.

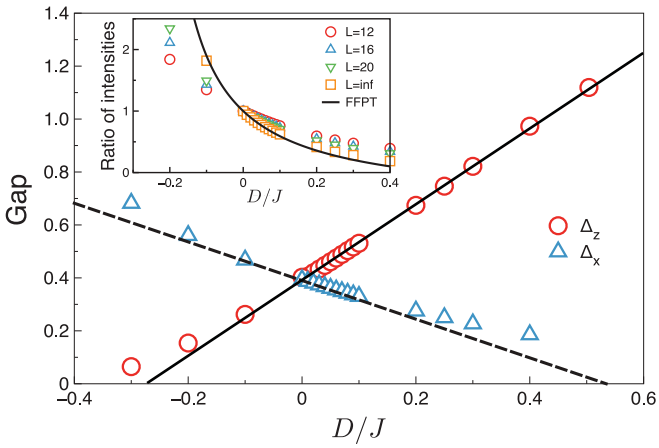


FIG. 2. (Color online) Numerically determined excitation gaps $\Delta_x$ (circles) and $\Delta_z$ (triangles) are plotted for $-0.4 \leqslant D/J \leqslant 0.6$ and $E = 0$. Deviation of the numerical data from the first-order FFPT (solid and dashed lines) is attributed to higher-order perturbations. Inset: The ratio $\mathcal{S}^{zz}(\pi,\Delta_z)/\mathcal{S}^{xx}(\pi,\Delta_x)$ obtained by the Lanczos method (symbols) and (14) (solid curve) are compared. The extrapolation to $L = \infty$ is done by fitting the finite-size data for $L = 12$, 14, 16, 18, and 20 with a polynomial of $1/L$.

Let us extend our discussion to the system under a finite magnetic field. Now our Hamiltonian $\mathcal{H} = \mathcal{H}_0 + \mathcal{H}_Z + \mathcal{H}'$ consists of three terms. $\mathcal{H}_0$ is the SU(2) symmetric exchange interaction, $\mathcal{H}_Z = -g_e\mu_B \boldsymbol{H}\cdot\boldsymbol{S} = -g_e\mu_B \boldsymbol{H}\cdot\sum_j \boldsymbol{S}_j$ is the Zeeman interaction, and $\mathcal{H}'$ is the SIA, which is assumed to be small. $g_e$ is Landé $g$ factor of electrons and $\mu_B$ is the Bohr magneton. We set $g_e\mu_B = 1$ unless otherwise stated. ESR is a very powerful tool to study the effects of anisotropies on spin dynamics. One of the fundamental quantities in ESR is the resonance frequency shift (ESR shift). The ESR shift is generally given, in the first order of the anisotropy $\mathcal{H}'$, as[24–26]

$$\delta\omega = -\frac{\langle[[\mathcal{H}',S^+],S^-]\rangle_0}{2\langle S^z\rangle_0}. \tag{15}$$

$\langle\cdots\rangle_0$ denotes the average with respect to the unperturbed Hamiltonian $\mathcal{H}^{(0)} = \mathcal{H}_0 + \mathcal{H}_Z$. For the SIA, (15) reads $\delta\omega = f(\Theta,\Phi)\,Y_D(T,H)$, where $f(\Theta,\Phi) = D(1 - 3\cos^2\Theta) - 3E\sin^2\Theta\cos 2\Phi$ and

$$Y_D(T,H) = \frac{\sum_j \langle 3(S_j^z)^2 - 2\rangle_0}{2\langle S^z\rangle_0}. \tag{16}$$

$(\Theta,\Phi)$ is the polar coordinate of the magnetic field axis.

To apply the results of the FFPT, first we consider the limit $T, H \ll \Delta_0$. Here we could project the numerator to a one-magnon subspace, ignoring the multimagnon contributions. The projection operator is $P_1 = \int \frac{d\theta}{4\pi}\sum_{a=0,\pm}|\theta,a\rangle\langle\theta,a|$. Note that we introduce a different set of indices $a = 0,\pm$ representing magnons with dispersion $E_a(\theta) = \Delta_0\cosh\theta - aH$. The projection leads to

$$P_1\sum_j\left[3(S_j^z)^2 - 2\right]P_1 = \int\frac{d\theta}{4\pi}\frac{3Z_2 v}{2\Delta_0\cosh\theta}[2|\theta,0\rangle\langle\theta,0| - |\theta,+\rangle\langle\theta,+| - |\theta,-\rangle\langle\theta,-|]. \tag{17}$$

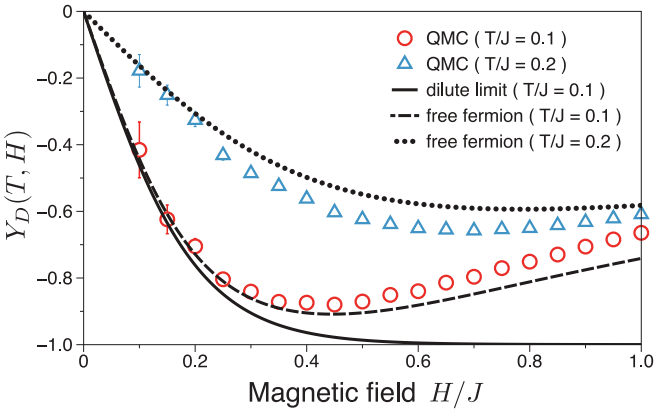


FIG. 3. (Color online) Magnetic field dependence of ESR shift $Y_D(T,H)$ for $T = 0.1J$ (circles) and $T = 0.2J$ (triangles). The solid curve is (18), which is exact in $H \to 0$. The dashed and dotted curves are (19) at $T = 0.1J$ and $T = 0.2J$, respectively.

Its thermal expectation value can be given in terms of the (classical) distribution function. Thus we find

$$Y_D(T,H) = -\frac{3Z_2}{4}\tanh\left(\frac{H}{2T}\right)\frac{\int \frac{d\theta}{4\pi}\frac{v}{\Delta_0\cosh\theta}e^{-\Delta_0\cosh\theta/T}}{\int \frac{d\theta}{4\pi}e^{-\Delta_0\cosh\theta/T}}. \tag{18}$$

Figure 3 shows the magnetic field dependence of $Y_D(T,H)$, comparing (18) from the FFPT with numerical results obtained by (16) with the quantum Monte Carlo (QMC) method in ALPS software.[27]

Although the agreement is good at low temperature $T = 0.1J$ and at low magnetic fields $H \ll \Delta_0$, the discrepancy is evident for $H \gtrsim \Delta_0$. This is rather natural, because the magnon population increases as $H$ is increased, invalidating the dilute limit approximation made in the derivation of Eq. (18). In particular, $T = 0$, $H = \Delta_0$ is a quantum critical point which separates the low-field gapped phase and the high-field TLL phase, where magnons are condensed. Although it is difficult to handle the case with nondilute magnons, a reasonable improvement would be incorporating magnon-magnon repulsion through the Pauli exclusion principle by utilizing the Fermi-Dirac distribution function $f_a(k) = [e^{\omega_a(k)/T} + 1]^{-1}$ instead of the classical one, in Eq. (18). This is demonstrated by the fact that the $z = 2$ free-fermion theory well describes the low-energy behavior near the quantum critical point $H = \Delta_0$.[28,29] The magnetization is $\langle S^z\rangle = m(T,H) = \int \frac{dk}{2\pi}[f_+(k) - f_-(k)]$ and $Y_D(T,H)$ is

$$Y_D(T,H) = \frac{3Z_2}{2m(T,H)}\int\frac{dk}{2\pi}\frac{v}{2\omega_0(k)} \times [2f_0(k) - f_+(k) - f_-(k)]. \tag{19}$$

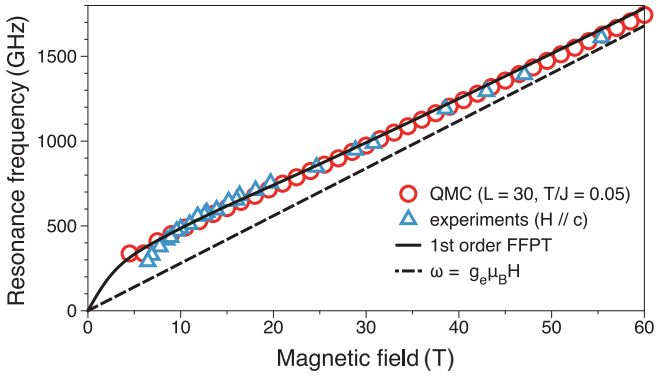


FIG. 4. (Color online) Comparison of the resonance frequency $\omega_r = g_e\mu_B H + \delta\omega$ by QMC (circles) with experimental data (Ref. 30) (triangles). We performed QMC calculations with $L = 30$ sites. We used $D = 0.25J$ and $H \parallel c$ ($\Theta = \Phi = 0$). The solid curve is obtained from (19) and the dashed line represents the paramagnetic resonance $\omega = g_e\mu_B H$.

This reduces to Eq. (18) in the limit $H, T \to 0$. We emphasize that there is no free parameter in our theory since the renormalization factor $Z_2$ in the overall coefficient of (19) has been already determined in (8). As shown in Fig. 3, the free-fermion approximation (19) explains the extremum of the ESR shift observed numerically around the critical field $H = \Delta_0$.

Figure 4 shows the ESR shift observed experimentally in $Ni(C_5H_{14}N_2)_2N_3(PF_6)$,[30] which possesses the SIA, and the corresponding numerical result by the QMC method. Our FFPT (19) successfully accounts for the experimental and numerical results, including the gradual approach to the paramagnetic resonance line $\omega = g_e\mu_B H$ in the high-field region. A detailed analysis of the ESR shift in the whole range of $H$ will be given in a subsequent publication.[31]

We thank Seiichiro Suga for giving us the motivation for this study. This work is partly supported by Grant-in-Aid for Scientific Research No. 21540381 (M.O.), the Global COE Program "The Physical Sciences Frontier" (S.C.F.), both from MEXT, Japan, and Grant-in-Aid from JSPS (Grant No. 09J08714) (S.T.). M.O. also acknowledges the Aspen Center for Physics where a part of this work was carried out (supported by US NSF Grant No. 1066293). We thank the ALPS project for providing the QMC code. Numerical calculations were performed at the ISSP Supercomputer Center of the University of Tokyo.

[1] T. Giamarchi, *Quantum Physics in One Dimension* (Oxford University Press, Oxford, UK, 2004).
[2] F. D. M. Haldane, Phys. Lett. A **93**, 464 (1983).
[3] I. Affleck, J. Phys. Condens. Matter **1**, 3047 (1989).
[4] I. Affleck, Phys. Rev. B **43**, 3215 (1991).
[5] I. Affleck, Phys. Rev. B **46**, 9002 (1992).
[6] F. H. L. Essler and I. Affleck, J. Stat. Mech. (2004) P12006.
[7] M. Karowski and P. Weisz, Nucl. Phys. B **139**, 455 (1978).

[8]B. Berg, M. Karowski, and P. Weisz, Phys. Rev. D **19**, 2477 (1979).
[9]F. A. Smirnov, *Form Factors in Completely Integrable Models of Quantum Field Theory* (World Scientific, Singapore, 1992).
[10]F. H. L. Essler and R. M. Konik, in *From Fields to Strings: Circumnavigating Theoretical Physics*, edited by M. Shifman, A. Vainshtein, and J. Wheater (World Scientific, Singapore, 2005).
[11]A. B. Zamolodchikov and A. B. Zamolodchikov, Nucl. Phys. B **133**, 525 (1978).
[12]M. D. P. Horton and I. Affleck, Phys. Rev. B **60**, 11891 (1999).
[13]F. H. L. Essler, Phys. Rev. B **62**, 3264 (2000).
[14]S. R. White and I. Affleck, Phys. Rev. B **77**, 134437 (2008).
[15]E. S. Sørensen and I. Affleck, Phys. Rev. B **49**, 13235 (1994); **49**, 15771 (1994).
[16]I. Affleck and R. A. Weston, Phys. Rev. B **45**, 4667 (1992); R. M. Konik, *ibid*. **68**, 104435 (2003).
[17]J. Balog and P. Weisz, Nucl. Phys. B **778**, 259 (2007).
[18]G. Vidal, Phys. Rev. Lett. **98**, 070201 (2007).
[19]S. Todo and K. Kato, Phys. Rev. Lett. **87**, 47203 (2001).
[20]H. Bergknoff and H. B. Thacker, Phys. Rev. D **19**, 3666 (1979).
[21]D. Controzzi and G. Mussardo, Phys. Rev. Lett. **92**, 021601 (2004).
[22]A. LeClair and G. Mussardo, Nucl. Phys. B **552**, 624 (1999).
[23]T. Suzuki and S.-i. Suga, Phys. Rev. B **72**, 014434 (2005).
[24]J. Kanamori and M. Tachiki, J. Phys. Soc. Jpn. **17**, 1384 (1962).
[25]K. Nagata and Y. Tazuke, J. Phys. Soc. Jpn. **32**, 337 (1972).
[26]Y. Maeda and M. Oshikawa, J. Phys. Soc. Jpn. **74**, 283 (2005).
[27]A. Albuquerque, F. Alet, P. Corboz, P. Dayal, A. Feiguin, S. Fuchs, L. Gamper, E. Gull, S. Gürtler, A. Honecker, R. Igarashi, M. Körner, A. Kozhevnikov, A. Läuchli, S. Manmana, M. Matsumoto, I. McCulloch, F. Michel, R. Noack, G. Pawlowski, L. Pollet, T. Pruschke, U. Schollwöck, S. Todo, S. Trebst, M. Troyer, P. Werner, and S. Wessel, J. Magn. Magn. Mater. **310**, 1187 (2007).
[28]H. J. Schulz, Phys. Rev. B **22**, 5274 (1980).
[29]Y. Maeda, C. Hotta, and M. Oshikawa, Phys. Rev. Lett. **99**, 57205 (2007).
[30]T. Kashiwagi, M. Hagiwara, S. Kimura, Z. Honda, H. Miyazaki, I. Harada, and K. Kindo, Phys. Rev. B **79**, 024403 (2009).
[31]S. C. Furuya, Y. Maeda, and M. Oshikawa (unpublished).